Biosensors and Bioelectronics 154 (2020) 112065

Contents lists available at ScienceDirect

Biosensors and Bioelectronics

journal homepage: http://www.elsevier.com/locate/bios

A surface plasmon resonance biosensor in conjunction with a DNA aptamer-antibody bioreceptor pair for heterogeneous nuclear ribonucleoprotein A1 concentrations in colorectal cancer plasma solutions

Sang Hyuk Lee [a], Yae Eun Park [b], Ji Eun Lee [b,**], Hye Jin Lee [a,*]

[a] Department of Chemistry and Green-Nano Materials Research Center, Kyungpook National University, 80 Daehakro, Buk-gu, Daegu-city, 41566, Republic of Korea
[b] Center for Theragnosis, Biomedical Research Institute, Korea Institute of Science and Technology, 5, Hwarang-ro 14-gil, Seongbuk-gu, Seoul, 02792, Republic of Korea

ARTICLE INFO

Keywords:
Surface sandwich assay
HnRNP A1
DNA aptamer/antibody bioreceptor pair
Surface plasmon resonance
Colorectal cancer
Human plasma

ABSTRACT

A new DNA aptamer and antibody pair was incorporated into surface plasmon resonance (SPR) sensing platform to detect heterogeneous nuclear ribonucleoprotein A1 (hnRNP A1) in plasma at clinically relevant native concentrations for the diagnosis of colorectal cancer (CRC). SPR detection of hnRNP A1 was realized via formation of the surface sandwich complex of aptamer/hnRNP A1/anti-hnRNP A; the specific adsorption of hnRNP A1 onto a gold chip surface modified with a DNA aptamer followed by the adsorption of anti-hnRNP A1. Changes in the refractive unit (RU) with respect to the hnRNP A1 concentration in buffer solutions were monitored at a fixed anti-hnRNP A1 concentration of 90 nM, resulting in a dynamic range of 0.1–10 nM of hnRNP A1. The surface sandwich SPR biosensor was further applied to the direct analysis of undiluted human normal and pooled CRC patient plasma solutions. Our plasma analysis results were compared to those obtained with a commercial enzyme-linked immunosorbent assay kit.

1. Introduction

Biomarkers in the human body, including proteins, nucleic acids, and metabolites, have been extensively investigated due to their widespread use in disease diagnosis (Park et al., 2018). In particular, decreased or elevated protein biomarker concentrations in biological fluids have been used as diagnostic indicators of cancer (Brinkman, 2004; Rusling et al., 2010), heart failure (Dhingra and Vasan, 2017), and Alzheimer's disease (Kim et al., 2018a; Medina-Sanchez et al., 2014). Colorectal cancer (CRC) is known to be one of the major diseases with a high death rate, majorly due to few noticeable symptoms. While there are several screening methods for CRC diagnosis (see Table S1), including colonoscopy (Kahi et al., 2013; Pickhardt et al., 2011; Sali et al., 2013, 2016), fecal occult blood test (Burch et al., 2007; La Vecchia, 2002), and magnetic resonance imaging (MRI) (Georgiou et al., 2013; Saunders et al., 2002), these tests are generally expensive, invasive, and may be accompanied by pain. Use of biomarkers for the diagnosis and prognosis of CRC could expedite treatment, which might increase the survival rate of CRC patients (Ma et al., 2009; Toma et al., 2018).

Extensive research efforts have been devoted to developing cost-effective and rapid diagnostic tools for the quantitative detection of disease-specific biomarkers. A wide range of sensing methodologies have been reported, which includes enzyme-linked immunosorbent assays (ELISAs), lateral flow immunoassays (Kim et al., 2018b), electrochemical assays (Diba et al., 2015; Lim et al., 2017; Westenbrink et al., 2015), and optical platforms (Liu et al., 2018; Ribaut et al., 2017). Surface plasmon resonance (SPR) is a surface sensitive technique that provides a label-free detection platform for various target protein biomarkers (He et al., 2017; Piliarik et al., 2010). The sensitivity of SPR for disease biomarkers have been improved by incorporation of biofunctionalized metallic nanoparticles (Wu et al., 2019; Zhao et al., 2019). One of the hurdles facing SPR is selectivity, because any non-specific adsorption of undesired molecules on the SPR sensing surface can elicit a response. Such a problem has been resolved by incorporating a pair of bioreceptors including either a DNA aptamer-antibody or an antibody-antibody for a target protein in the

* Corresponding author. Department of Chemistry and Green-Nano Materials Research Center, Kyungpook National University, 80 Daehakro, Buk-gu, Daegu-city, 41566, Republic of Korea.
** Corresponding author. Center for Theragnosis, Biomedical Research Institute, Korea Institute of Science and Technology, 5, Hwarang-ro 14-gil, Seongbuk-gu, Seoul, 02792, Republic of Korea.
E-mail addresses: jelee9137@kist.re.kr (J.E. Lee), hyejinlee@knu.ac.kr (H.J. Lee).

https://doi.org/10.1016/j.bios.2020.112065
Received 27 November 2019; Received in revised form 25 January 2020; Accepted 27 January 2020
Available online 29 January 2020

sensing platform (Jang et al., 2014; Kim and Lee, 2015, Kim et al., 2016, 2017b).

While several protein biomarkers specific to CRC, including human leukocyte antigen-G (Cao et al., 2011), adipophilin (Matsubara et al., 2011), interleukin 8 (Fung et al., 2015), and matrix remodeling-associated 5 (Wang et al., 2013), have been reported, heterogeneous nuclear ribonucleoprotein A1 (hnRNP A1) was also discussed as a potential biomarker for CRC (Ma et al., 2009). However, there have been only few reports available for quantification of hnRNP A1 using real-time polymerase chain reaction, western blotting, and ELISA (Boukakis et al., 2010; Ke et al., 2018; Ma et al., 2009; Park et al., 2016) (see Table S2), and more importantly not yet been incorporated into a quantitative SPR analysis for CRC diagnosis. Herein we report for the first time a new pair of DNA aptamer and antibody integrated into a surface sandwich assay platform for detection of hnRNP A1 using real-time SPR analysis. Strong binding affinities of both bioreceptors toward hnRNP A1 were first confirmed using SPR. A clinically relevant nanomolar concentration range for hnRNP A1 was then established for the sandwich assay platform formed via the sequential adsorption of hnRNP A1 and anti-hnRNP A1 onto a surface tethered DNA aptamer on a SPR chip. Our SPR sandwich assay was finally applied to direct measurements of hnRNP A1 concentrations in undiluted normal and pooled CRC plasma samples of which results were compared to those obtained from a commercial ELISA kit.

2. Experimental section

2.1. Materials

Recombinant human hnRNP A1 full length protein (hnRNP A1, 37 kDa, Abcam, ab123212), hnRNP A1 antibody (anti-hnRNP A1, 150 kDa, Abcam,ab5832), recombinant human retinol binding protein 4 (RBP4, 22 kDa, R&D Systems), retinol binding protein 4 antibody (anti-RBP4, 150 kDa, R&D Systems), human plasma (Sigma-Aldrich), hnRNP A1 ELISA kit (sandwich assay type, Cusabio Biotech, Co. Ltd., Wuhan, PR China), Amicon®Ultra centrifugal filter 100 K (UFC510024, Millipore), (1-ethyl-3-(3-dimethylaminopropyl)carbodiimde hydrochloride (EDC, Thermo), *N*-hydroxysulfosuccinimide (NHSS or Sulfo-NHS, Thermo), 11-mercaptoundecanoic acid (MUA, Sigma-Aldrich), and 11-mercaptoundecanol (MUD, Sigma-Aldrich) were all used as received. A 5′-amine modified DNA aptamer specific to hnRNP A1 (Zhang et al., 2015), whose sequence is 5'-H_2N-GCA ATG GTA CGG TAC TTC CTG TGG CGA GGT AGG TGG GGT GTG TGT GTA TCC AAA AGT GCA CGC TAC TTT GCT AA-3′, and a negative control (NC4) sequence, 5′-H_2N-ATA CCA GCT TAT TCA ATT ACA GTA GTG AGG GGT CCG TCG TGG GGT AGT TGG GTC GTG GAG ATA GTA AGT GCA ATC T-3′ specific to RBP4 (Lee et al., 2008), were purchased from IDT. All bioaffinity measurements using SPR were performed in 1X phosphate-buffered saline (PBS) solution (pH 7.4, Life Technologies) or in human normal (Sigma-Aldrich) and CRC plasma samples pooled from eight CRC patients with stage III (Severance Hospital Gene Bank, Seoul, Korea). Authorization to use the CRC plasma samples was obtained from the Institutional Review Board of Severance Hospital. All binding measurements and fabrication of aptamer and antibody chips were performed at room temperature, otherwise specified.

2.2. Creation of aptamer or antibody modified SPR chips

A summary of the surface immobilization for attaching hnRNP A1 aptamers or anti-hnRNP A1 onto a monolayer of MUA-modified gold surface is shown in Scheme 1. Briefly, the bare SPR gold chip was immersed in 1 mM MUA (100% MUA) or mixed MUA and MUD (1:1) in ethanol with the total concentration fixed at 1 mM for 12 h followed by rinsing with ethanol and deionized (DI) water. The chip was then exposed to a mixture of 7.5 mM EDC and 1.5 mM sulfo-NHS solution for 20 min, providing a carboxylic acid terminated chip surface. Next, the chip was rinsed with DI water and then exposed to 1 mM hnRNP A1 aptamer or 6.67 μM anti-hnRNP A1 for a minimum of 3 h in a humidity chamber. The aptamer or antibody-tethered chip was finally rinsed with DI water and kept at room temperature prior to SPR measurements. The surface morphology and sandwich formation on the gold surface were further investigated using atomic force microscopy (AFM, Park Systems, NX-20) and scanning electron microscopy (SEM, HITACHI S-4100, and FEI XL-30 FEG).

2.3. SPR measurements

A Biacore 3000 was used for in situ monitoring of all biomolecular binding measurements (GE Healthcare, Chicago, USA). A running buffer of 1X PBS (pH 7.4) solution and a flow rate of 3 μL/min (protein) and 5 μL/min (antibody) were applied for all experiments. Different concentrations of hnRNP A1 in PBS solutions were individually injected over the aptamer or anti-hnRNP A1 functionalized SPR chip for a minimum of 1 h to assure a steady-state surface coverage of hnRNP A1 for all bioaffinity measurements. For real sample analyses, instead of injecting hnRNP A1 in PBS solution, either human (Sigma-Aldrich) or pooled CRC plasma sample solution, which was filtered using Amicon®Ultra filter (Millipore), was flowed over the surface for at least 1 h followed by washing with PBS solution. Freshly prepared SPR chip was used for measurements of plasma samples. Standard addition was performed for SPR analysis of real samples by spiking from 1.2 to 4.6 μL of the hnRNP A1 stock solution (500 nM) into plasma samples to make from 2.5 to 10 nM. Each reported Δ refractive unit (RU) value was obtained by measuring the RU value before exposing the aptamer/hnRNP A1 surface to an anti-hnRNP A1 solution and subtracting the value from the RU value measured after rinsing the surface of the aptamer/hnRNP A1/anti-hnRNP A1 sandwich complex with PBS. Normalized RU values were obtained by subtracting the average Δ RU value of the non-specific binding control measurements from the average Δ RU value recorded during the specific hnRNP A1 binding events. For the sandwich assay, a fixed concentration (90 nM) of anti-hnRNP A1 in PBS (pH 7.4) solution was injected onto the DNA aptamer/hnRNP A1 complex for 40 min followed by washing with PBS for 10 min. For non-specific binding measurements, different concentrations of RBP4 (NC2) and anti-RBP4 (NC3) alongside the non-interacting aptamer sequence (NC4) immobilized on the chip surface were used. Different μL aliquots of stock solution (500 nM) of hnRNP A1 were directly added to either human normal or pooled CRC plasma sample solution for spiking experiments of

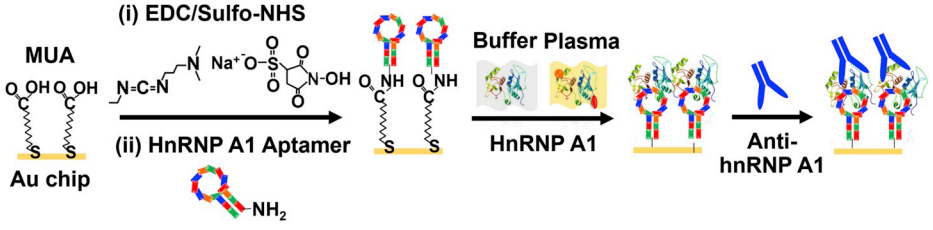

Scheme 1. Schematic overview of the SPR detection process for hnRNP A1 via formation of the surface sandwich complex of DNA aptamer/hnRNP A1/anti-hnRNP A1. Briefly, a self-assembled MUA monolayer on a thin gold SPR chip was modified with a covalently bound hnRNP A1 specific DNA aptamer using EDC/sulfo-NHS chemistry. Specific adsorption of hnRNP A1 in both PBS and plasma solutions onto the DNA aptamer-coated surface was monitored along with the subsequent binding of anti-hnRNP A1.

known concentrations of hnRNP A1 in PBS.

3. Results and discussion

3.1. Detection of the HnRNP A1 using SPR

HnRNP A1, which is known as a versatile binding protein for single-stranded nucleic acid (Ding et al., 1999), was suggested as a biomarker for CRC, because the concentrations of the protein in serum samples from CRC patients were found to be elevated relative to those in control samples using ELISA experiments (Ma et al., 2009). However, there has not yet been a SPR sensing platform for detection of hnRNP A1 in clinical samples. In our present study, a surface sandwich assay strategy using a DNA aptamer and antibody particularly targeting for detection of hnRNP A1 in Scheme 1 is for the first time introduced, which can be potentially utilized for CRC diagnosis. Such sandwich assay platforms could contribute to an enhancement in the selectivity and controlling SPR signal amplification (Jang et al., 2014; Kim and Lee, 2015, Kim et al., 2016, 2018c, Kim and Lee, 2017). An alkane thiol with a carboxylic acid terminal group (MUA) was self-assembled on a bare gold SPR chip surface followed by the covalent attachment with an amine modified DNA aptamer probe (1 mM) specific to hnRNP A1 using EDC/sulfo-NHS linking chemistry. This process was monitored using a real-time SPR shown in Fig. S1 demonstrating that the aptamer immobilization process required a minimum of 20 min. Sequential exposure of the SPR chip to hnRNP A1 and anti-hnRNP A1 resulted in the formation of the DNA aptamer/hnRNP A1/anti-hnRNP A1 sandwich complex on the surface. Adsorption of hnRNP A1 at different concentrations in PBS solution was monitored using a real-time SPR analysis to establish the feasibility of the proposed sandwich assay prior to the direct analysis of hnRNP A1 in human plasma samples.

Prior to using the sandwich assay for hnRNP A1, binding strengths of each immobilized probe, DNA aptamer and anti-hnRNP A1 on the gold chip, respectively, modified with 100% MUA were investigated by monitoring adsorption of hnRNP A1 in PBS solution at various concentrations. The mixture of MUA and MUD (1:1) prior to attachment of DNA aptamer or anti-hnRNP A1 to adjust the surface probe density was also studied. The corresponding RU changes from SPR sensorgrams (Fig. S2) were first plotted as a function of hnRNP A1 concentration. These plots were then utilized to generate plots of the fractional surface coverage (θ) with respect to the target concentration. The θ value at each hnRNP A1 concentration was calculated by dividing Δ RU value at each hnRNP A1 concentration (C) by Δ RU value for maximum binding of the target protein to either the DNA aptamer or the anti-hnRNP A1 tethered to the chip surface. The SPR results were fitted with the Langmuir adsorption isotherm model (eq. (1)) developed for a simple 1:1 binding between a target and a ligand tethered to the surface without additional interactions between adsorbed molecules (Kim and Lee, 2015).

$$\theta = \frac{K_{ads}C}{1 + K_{ads}C} \quad (1)$$

where K_{ads} is the hnRNP A1 adsorption coefficient (M^{-1}) of the ligand. K_{ads} values were 2.36 (±0.16) × 10^7 M^{-1} and 1.77 (±0.17) × 10^7 M^{-1}, respectively, when using the DNA aptamer and anti-hnRNP A1 attached onto a 100% MUA modified gold surface (see Fig. 1). The K_{ads} of our DNA aptamer was reasonable when compared to the equilibrium dissociation constant (K_D) of 111.0 ± 36.9 nM reported by Li et al. (2009). The strong binding affinity of anti-hnRNP A1 for hnRNP A1 suggested by our K_{ads} was consistent with previously reported western blotting measurements (Li et al., 2009, 2018; Ma et al., 2009). When the surface density of the immobilized probe was lowered using a mixed 1:1 ratio of MUA:MUD, smaller SPR signals compared to those of using 100% MUA monolayer further resulted in reducing the binding constants of both DNA and anti-hnRNP A1 towards hnRNP A1 as 1.34 (±0.04) × 10^7 M^{-1} and 0.69 (±0.04) × 10^7 M^{-1}, respectively Fig. 1.

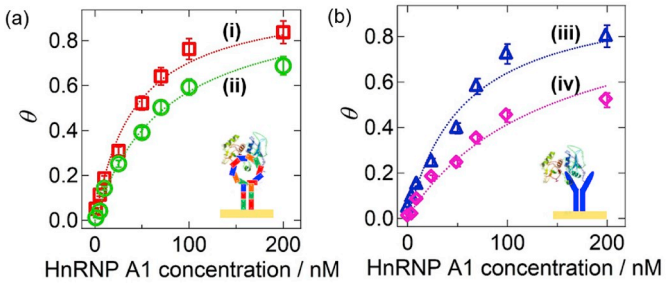

Fig. 1. Langmuir adsorption isotherms showing fractional surface coverage (θ) as a function of hnRNP A1 concentration on (a) DNA aptamer and (b) anti-hnRNP A1 probes where (i) and (iii) were created on a 100% MUA-modified and (ii) and (iv) on a mixed monolayer of MUA:MUD (1:1) on gold chips. (For interpretation of the references to color in this figure legend, the reader is referred to the Web version of this article.)

The DNA aptamer was chosen as the probe attached to the surface due to its higher binding strength toward the hnRNP A1 in addition to robust and precise control over packing density and non-specific adsorption, whereas the anti-hnRNP A1 was used as a detection probe when configuring a surface sandwich assay for analysis of hnRNP A1. We next determined whether the two bioreceptors interacted with different epitopes on the hnRNP A1 to enable sandwich complex formation. Full surface coverage by the target bound to the DNA aptamer was achieved at a fixed hnRNP A1 concentration of 100 nM (Fig. S3), which was injected over the chip surface tethered with the DNA aptamer. The surface was then exposed to different concentrations of anti-hnRNP A1. The resulting RU signal increased as the anti-hnRNP A1 concentration increased, confirming that the aptamer-antibody pair was able to form a surface sandwich complex with hnRNP A1.

Negligible changes in the responses were observed at concentrations of the detection probe of anti-hnRNP A1 above 200 nM due to the saturation of SPR signal. The increment in SPR response as the sequential adsorption of the target and anti-hnRNP Al onto the surface modified with the aptamer provides a hint for the formation of surface sandwich complexes, which was further investigated using AFM (Fig. S4) and SEM analyses (Fig. S5). Both data were taken ex-situ where each chip was dried prior to the measurements, which could cause the loss of bioactivity and the formation of unwanted clusters, resulting in errors in accurate estimation of the thickness of the sandwich complex. Compared to the bare chip, surface morphologies were changed and thicker layers were built for both aptamer and sandwich complexes on the chips. A thicker layer was observed as the number of adsorption steps (aptamer only versus aptamer/hnRNP A1/anti-hnRNP A1) increased, which confirms that the adsorption of hnRNP A1 and anti-hnRNP A1 occurred on the aptamer layer. It should also be noted that there are some regions containing clusters of salt around the sandwich complexes on the chip, which may come from buffer elements used for the binding events of hnRNP A1 and anti-hnRNP A1. In-situ AFM or other in-situ surface sensitive techniques could be further employed to validate the formation of sandwich complex in a nanometer range.

3.2. Sandwich assay

Confirming that both DNA aptamer and anti-hnRNP A1 interact with the different epitopes of the target protein allows us to configure a surface sandwich assay for measuring hnRNP A1 concentrations in buffer. A series of representative real-time SPR measurements for the adsorption of 90 nM anti-hnRNP A1 onto the different concentrations of hnRNP A1 are shown in Fig. 2a and Fig. S6 alongside Fig. S7 featuring SPR sensorgrams for the whole adsorption process. The SPR responses increased as the injected concentrations of hnRNP A1 increased followed by the anti-hnRNP A1, which demonstrates the sequential adsorption events for formation of a sandwich complex.

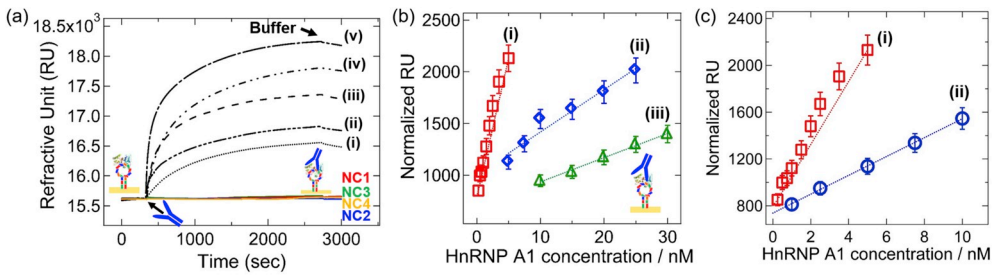

Fig. 2. Representative real-time SPR responses to hnRNP A1 at various concentrations using chips functionalized with a hnRNP A1 specific DNA aptamer and a fixed concentration of anti-hnRNP A1 (90 nM). (a) Representative SPR sensorgrams at injected hnRNP A1 concentrations of (i) 0.25 nM, (ii) 1 nM, (iii) 2.5 nM, (iv) 5 nM, and (v) 10 nM. NC1-4 represent the negative control measurements (See Table 1). (b) Plots of the normalized RU values as a function of hnRNP A1 concentrations using DNA aptamer probes attached onto 100% MUA-modified surface. The anti-hnRNP A1 concentrations were (i) 90, (ii) 80, and (iii) 40 nM. (c) Plots of the normalized RU values as a function of hnRNP A1 concentration using DNA aptamer probes attached onto (i) a 100% MUA and (ii) mixed MUA:MUD (1:1) monolayer surface. A fixed concentration of hnRNP A1 at 90 nM was used. The linear response range in each series (b) and (c) is indicated by a dotted line.

Further experiments to select anti-hnRNP A1 concentration for establishing the sensitivity and dynamic range of hnRNP A1 concentrations were performed by comparing the normalized RU values measured as a function of hnRNP A1 concentrations in the buffer at fixed concentrations (40, 80, and 90 nM) of anti-hnRNP A1. The RU values were normalized by subtracting the average Δ RU value of negative controls (NC1-NC4, see Table 1) from Δ RU values recorded as the anti-hnRNP A1, forming the sandwich complex with hnRNP A1 bound to the aptamer in order to consider the SPR signals due to non-specific adsorption of undesired proteins or antibodies onto the DNA aptamer surface. Each NC component is shown schematically in Table 1 where NC1 indicates the SPR signal measured in the absence of hnRNP A1, while NC2 indicates adsorption of one of the proteins present in plasma (RBP4). NC3 represents SPR measurement when anti-hnRNP A1 is replaced by anti-RBP4. NC4 indicates the use of an aptamer sequence that differs from that of the hnRNP A1 specific sequence.

Obviously, the sensitivity value was enhanced as 23.4, 40.9, and 278.3 normalized RU/nM when the detection probe of anti-hnRNP A1 concentration increased as 40, 80, and 90 nM, respectively, while the dynamic ranges were varied from 10-30 nM, 5–25 nM, and 0.25–5 nM, respectively (Fig. 2b). Since clinically relevant concentrations of hnRNP A1 as a biomarker for the diagnosis of CRC is in the range of 0.9–3.11 nM (Ma et al., 2009), a fixed concentration of 90 nM anti-hnRNP A1 was chosen to establish quantitative analyses of hnRNP A1 in buffer. In this case, the lowest detectable hnRNP A1 concentration was ~0.1 nM (Fig. S6), a linear dynamic range was established from 0.25 to 5 nM with limit of detection (LOD) value of 0.22 nM. The observed sensitivity for our sandwich assay format was higher than that for the hnRNP A1 adsorbed solely to the DNA aptamer (5.18 normalized RU/nM).

In addition, the effect of aptamer density on the sensitivity was studied where the SPR signal response using a mixed MUA:MUD and a 100% MUA monolayer for attachment of DNA aptamer was plotted as a function of hnRNP A1 at a 90 nM anti-hnRNP A1 (see Fig. 2c). The sensitivity of the diluted aptamer chip (80.5 normalized RU/nM) decreased almost 1/3 times compared to that using the aptamer chip created on 100% MUA (278.3 normalized RU/nM). An excellent long-term stability was achieved by obtaining almost identical RU signal for detecting 1 nM of hnRNP A1 in the sandwich format using three different aptamer chips individually kept for 1 month at room temperature (Fig. S8).

Table 1
Summary of four different negative control (NC) measurements from reference SPR chip channels. These were used to normalize signals from the hnRNP A1 detection channel during the anti-hnRNP A1 binding stage in buffer and plasma. NC1 indicates the SPR signal measured in the absence of hnRNP A1, while NC2 indicates adsorption of one of the proteins present in plasma (RBP4). NC3 represents SPR measurement when anti-hnRNP A1 is replaced by anti-RBP4. NC4 indicates the use of an aptamer sequence that differs from that of the hnRNP A1 specific sequence.

	NC1	NC2	NC3	NC4
Aptamer	HnRNP A1 sequence			Control sequence
Protein	None	RBP4	HnRNP A1	
Antibody	Anti-hnRNP A1		Anti-RBP4	Anti-hnRNP A1
Scheme	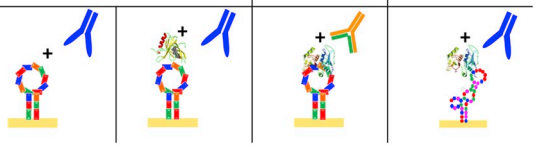			

3.3. Measurement of hnRNP A1 concentrations in plasma

After confirming that the concentration of hnRNP A1 in PBS solution could be determined using our surface sandwich SPR bioassay, a series of direct SPR measurements were performed in undiluted normal and pooled CRC plasma samples. SPR sensorgrams, respectively, obtained from the injection of normal and pooled CRC plasma solutions onto the DNA apmater-modified chip surface were shown in Fig. S9 and also plasma samples spiked with hnRNP A1 to concentrations ranging from 2.5 nM to 10 nM in Fig. 3a and b. A 90 nM anti-hnRNP Al concentration was employed to establish the linear dynamic detection range for hnRNP A1 at nanomolar concentrations. RU values obtained from hnRNP A1 measurements in PBS solutions were larger than those recorded at the same protein concentrations after spiking into normal and pooled CRC plasma. Also the sensitivity for normal (35.38 Δ RU/nM) and pooled CRC plasma (55.63 Δ RU/nM) spiked with hnRNP A1 was between 2.5 nM and 10 nM, which was almost 5–7 times lower to that in buffer solution (278.3 normalized RU/nM), implying that there are background signals from the plasma which were caused mainly by non-specific binding of proteins in the human plasma samples to DNA aptamers tethered to the chip surface, which can be seen from the real-time SPR response for undiluted normal and pooled CRC plasma sample itself adsorbing onto the aptamer surface (Fig. S9). This would reduce the

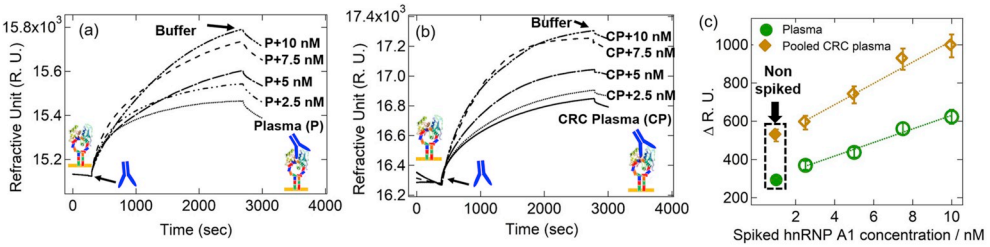

Fig. 3. A series of real-time SPR measurements of (a) normal and (b) pooled CRC plasma (CP) samples using chips functionalized with the hnRNP A1 specific DNA aptamer. A fixed anti-hnRNP A1 concentration of 90 nM was used in all experiments. Plasma samples were spiked with hnRNP A1 to concentrations of 2.5, 5, 7.5, or 10 nM. (c) Δ RU values from the datasets in (a) and (b) versus the spiked hnRNP A1 concentration. The linear response range for each dataset is indicated by the dotted line. The filled circles and squares represent normal and pooled CRC plasma samples, respectively.

number of DNA aptamers available to hnRNP A1, which would lead to a subsequent decrease in the amount of anti-hnRNP A1 on the chip surface.

Representative plots of Δ RU as a function of the known hnRNP A1 spiking concentration for both undiluted plasma samples are shown in Fig. 3c where the data of non-spiked plasma show the Δ RU of the plasma itself. The native hnRNP A1 concentration in the undiluted normal plasma was estimated from the linear fit ($y = ax + b$) of the Δ RU values from the spiked dataset (Fig. 3c) using a y offset Δ RU value (b) of 276.6. After substituting the slope (35.38) and the y offset (b) in the linear equation, the native hnRNP A1 concentration was estimated to be 0.47 nM. The calculated slope and b value for the pooled CRC plasma were 55.63 and 464.1, respectively, yielding an estimated native hnRNP A1 concentration of 1.12 nM. These results appeared reasonable when compared to hnRNP A1 levels (0.96–3.11 nM) in the serum of CRC patients reported by Ma et al. (2009).

While our SPR plasma analyses were comparable to those reported by Ma et al. (2009), we further attempted to measure hnRNP A1 concentrations in plasma using a commercially available ELISA kit. The ELISA results are shown along with hnRNP A1 standard curves for a series of concentrations provided by the manufacturer in Fig. S10. The estimated native concentration level of hnRNP A1 in undiluted pooled CRC plasma sample using the ELISA kit was lower than that obtained from our SPR measurements, and also the protein concentration was not determinable for the normal plasma solution with the ELISA. Such a dissimilarity in estimating hnRNP A1 concentration in both plasma measurements could come from; (i) a difference in the dynamic range between ELISA (0.01–0.54 nM) and our SPR (0.25–5 nM in the PBS solution) sandwich assays (Fig. S11) where we intended to control the dynamic range for the SPR measurements by using a fixed concentration of the detection probe (i.e., antibody) within the reported clinically relevant nanomolar range (Ma et al., 2009), and (ii) a lower sensitivity for SPR measurements compared to that of ELISA mainly originated from unremovable non-specific adsorption events of undesired biomolecules in plasma sample solutions onto the aptamer surface contributing to errors in SPR measurements alongside the choice of concentration of our detection antibody probe. In addition, differences between anti-hnRNP A1 used for our SPR biosensor and ELISA could also contribute to the discrepancy in the results. Nevertheless, the use of blocking reagent such as MUD mixing with MUA when attaching the aptamer could be a potential solution for improving non-specific adsorption events, but the dilution of surface attached aptamer concentration could reduce the SPR signal. Further studies on controlling the aptamer surface more resistant to undesired biomolecules, but reserving high sensitivity will be underway.

4. Conclusions

A robust sandwich assay platform with a DNA aptamer and anti-hnRNP A1 pair as a surface and detection probe, respectively, in conjunction with a series of negative control measurements was reported for the first time to measure hnRNP A1 at nanomolar concentration ranges in both buffer and undiluted normal and pooled CRC plasma samples. Importantly, tailoring the concentration of the antibody detection probe enabled us to establish a dynamic range for the target biomarker at clinically relevant concentrations. Considering that few reports on SPR sensing with patient plasma samples are available, our plasma analysis results reasonably correlated to those reported in the literature (Ma et al., 2009) can provide a new route to develop biomedical applications using a SPR biosensor.

Declaration of competing interest

The authors declare that they have no known competing financial interests or personal relationships that could have appeared to influence the work reported in this paper.

CRediT authorship contribution statement

Sang Hyuk Lee: Data curation, Formal analysis, Writing - original draft, Investigation. **Yae Eun Park:** Data curation. **Ji Eun Lee:** Writing - review & editing, Methodology. **Hye Jin Lee:** Writing - review & editing, Conceptualization, Supervision.

Acknowledgements

This work was supported by the National Research Foundation (NRF) of Korea funded by the Ministry of Science, ICT, and Future Planning (Grant number: NRF-2019R1A2C1002710). Separately, Dr. J. Lee acknowledges a KIST institutional program.

Appendix A. Supplementary data

Supplementary data to this article can be found online at https://doi.org/10.1016/j.bios.2020.112065.

References

Boukakis, G., Patrinou-Georgoula, M., Lekarakou, M., Valavanis, C., Guialis, A., 2010. BMC Canc. 10, 434.
Brinkman, B.M.N., 2004. Clin. Biochem. 37, 584–594.
Burch, J.A., Soares-Weiser, K., St John, D.J., Duffy, S., Smith, S., Kleijnen, J., Westwood, M., 2007. J. Med. Screen 14, 132–137.
Cao, M., Yie, S.M., Liu, J., Ye, S.R., Xia, D., Gao, E., 2011. Tissue Antigens 78, 120–128.
Dhingra, R., Vasan, R.S., 2017. Trends Cardiovasc. Med. 27, 123–133.
Diba, F.S., Kim, S., Lee, H.J., 2015. Biosens. Bioelectron. 72, 355–361.
Ding, J., Hayashi, M.K., Zhang, Y., Manche, L., Krainer, A.R., Xu, R.M., 1999. Genes Dev. 13, 1102–1115.
Fung, K.Y., Tabor, B., Buckley, M.J., Priebe, I.K., Purins, L., Pompeia, C., Brierley, G.V., Lockett, T., Gibbs, P., Tie, J., McMurrick, P., Moore, J., Ruszkiewicz, A., Nice, E., Adams, T.E., Burgess, A., Cosgrove, L.J., 2015. PloS One 10, 1–11.
Georgiou, P.A., Tekkis, P.P., Constantinides, V.A., Patel, U., Goldin, R.D., Darzi, A.W., John Nicholls, R., Brown, G., 2013. Eur. J. Canc. 49, 72–81.
He, L., Pagneux, Q., Larroulet, I., Serrano, A.Y., Pesquera, A., Zurutuza, A., Mandler, D., Boukherroub, R., Szunerits, S., 2017. Biosens. Bioelectron. 89, 606–611.
Jang, H.R., Wark, A.W., Baek, S.H., Chung, B.H., Lee, H.J., 2014. Anal. Chem. 86, 814–819.
Kahi, C.J., Anderson, J.C., Rex, D.K., 2013. Gastrointest. Endosc. 77, 335–350.

Ke, R., Lv, L., Li, J., Zhang, X., Yang, F., Zhang, K., Jiang, Y., 2018. Oncol. Lett. 16, 3746–3756.
Kim, H., Lee, J.U., Song, S., Kim, S., Sim, S.J., 2018a. Biosens. Bioelectron. 101, 96–102.
Kim, J., Kwon, J.H., Jang, J., Lee, H., Kim, S., Hahn, Y.K., Kim, S.K., Lee, K.H., Lee, S., Pyo, H., Song, C.S., Lee, J., 2018b. Biosens. Bioelectron. 112, 209–215.
Kim, S., Lee, H.J., 2015. Anal. Chem. 87, 7235–7240.
Kim, S., Lee, H.J., 2017. Anal. Chem. 89, 6624–6630.
Kim, S., Lee, S., Lee, H.J., 2018c. Sensor. Actuator. B Chem. 273, 1029–1036.
Kim, S., Park, J.W., Wark, A.W., Jhung, S.H., Lee, H.J., 2017. Anal. Chem. 89, 12562–12568.
Kim, S., Wark, A.W., Lee, H.J., 2016. Anal. Chem. 88, 7793–7799.
La Vecchia, C., 2002. Ann. Oncol. 13, 31–34.
Lee, S.J., Youn, B.S., Park, J.W., Niazi, J.H., Kim, Y.S., Gu, M.B., 2008. Anal. Chem. 80, 2867–2873.
Li, L., Yang, X., Li, K., Zhang, G., Ma, Y., Cai, B., Li, S., Ding, H., Deng, J., Nan, X., Sun, J., Wu, Y., Shao, N., Zhang, L., Yang, Z., 2018. Org. Biomol. Chem. 16, 7488–7497.
Li, S., Xu, H., Ding, H., Huang, Y., Cao, X., Yang, G., Li, J., Xie, Z., Meng, Y., Li, X., Zhao, Q., Shen, B., Shao, N., 2009. J. Pathol. 218, 327–336.
Lim, J.M., Ryu, M.Y., Yun, J.W., Park, T.J., Park, J.P., 2017. Biosens. Bioelectron. 98, 330–337.
Liu, T., Liang, L.L., Xiao, P., Sun, L.P., Huang, Y.Y., Ran, Y., Jin, L., Guan, B.O., 2018. Biosens. Bioelectron. 100, 155–160.
Ma, Y.L., Peng, J.Y., Zhang, P., Huang, L., Liu, W.J., Shen, T.Y., Chen, H.Q., Zhou, Y.K., Zhang, M., Chu, Z.X., Qin, H.L., 2009. J. Proteome Res. 8, 4525–4535.
Matsubara, J., Honda, K., Ono, M., Sekine, S., Tanaka, Y., Kobayashi, M., Jung, G., Sakuma, T., Nakamori, S., Sata, N., Nagai, H., Ioka, T., Okusaka, T., Kosuge, T., Tsuchida, A., Shimahara, M., Yasunami, Y., Chiba, T., Yamada, T., 2011. Canc. Epidemiol. Biomarkers Prev. 20, 2195–2203.
Medina-Sanchez, M., Miserere, S., Morales-Narvaez, E., Merkoci, A., 2014. Biosens. Bioelectron. 54, 279–284.
Park, M., Kang, B.-H., Jeong, K.-H., 2018. Biochip. J. 12, 1–10.
Park, W.C., Kim, H.R., Kang, D.B., Ryu, J.S., Choi, K.H., Lee, G.O., Yun, K.J., Kim, K.Y., Park, R., Yoon, K.H., Cho, J.H., Lee, Y.J., Chae, S.C., Park, M.C., Park, D.S., 2016. BMC Canc. 16, 358.
Pickhardt, P.J., Hassan, C., Halligan, S., Marmo, R., 2011. Radiology 259, 393–405.
Piliarik, M., Bockova, M., Homola, J., 2010. Biosens. Bioelectron. 26, 1656–1661.
Ribaut, C., Loyez, M., Larrieu, J.C., Chevineau, S., Lambert, P., Remmelink, M., Wattiez, R., Caucheteur, C., 2017. Biosens. Bioelectron. 92, 449–456.
Rusling, J.F., Kumar, C.V., Gutkind, J.S., Patel, V., 2010. Analyst 135, 2496–2511.
Sali, L., Grazzini, G., Carozzi, F., Castiglione, G., Falchini, M., Mallardi, B., Mantellini, P., Ventura, L., Regge, D., Zappa, M., Mascalchi, M., Milani, S., 2013. Trials 14, 1–9.
Sali, L., Regge, D., 2016. Br. J. Radiol. 89, 20160517.
Saunders, T.H., Mendes Ribeiro, H.K., Gleeson, F.V., 2002. Br. Med. Bull. 64, 81–99.
Toma, S.C., Ungureanu, B.S., Patrascu, S., Surlin, V., Georgescu, I., 2018. Curr. Health Sci. J. 44, 140–146.
Wang, G.H., Yao, L., Xu, H.W., Tang, W.T., Fu, J.H., Hu, X.F., Cui, L., Xu, X.M., 2013. Oncol. Lett. 5, 544–548.
Westenbrink, E., Arasaradnam, R.P., O'Connell, N., Bailey, C., Nwokolo, C., Bardhan, K. D., Covington, J.A., 2015. Biosens. Bioelectron. 67, 733–738.
Wu, Q., Li, N., Wang, Y., Liu, Y., Xu, Y., Wei, S., Wu, J., Jia, G., Fang, X., Chen, F., Cui, X., 2019. Biosens. Bioelectron. 144, 111697.
Zhang, J., Li, S., Liu, F., Zhou, L., Shao, N., Zhao, X., 2015. PloS One 10, 1–9.
Zhao, J., Liang, D., Gao, S., Hu, X., Koh, K., Chen, H., 2019. Biosens. Bioelectron. 141, 111440.